Journal of Engineering Mathematics (2006) 54: 211–224
DOI 10.1007/s10665-005-9010-5

Similarity without diffusion: shear turbulent layer damped by buoyancy

D.V. STRUNIN
Department of Mathematics and Computing, University of Southern Queensland, Toowoomba, QLD 4350, Australia (E-mail: strunin@usq.edu.au)

Received 7 June 2004; accepted in revised form 15 July 2005 / Published online: 17 January 2006

Abstract. The evolution of a turbulent layer generated by velocity shear between two half-spaces of fluid and suppressed by a stable density difference is studied. Initially the layer expands, then shrinks to a point in finite time. By the end of the expansion stage the turbulent diffusion decays to a small value compared to the shear and buoyancy inputs in the turbulent energy balance. During the shrinking stage the diffusion decays even further by comparison. It is shown that at this stage the profiles of the turbulent energy, velocity and buoyancy become virtually self-similar. The differences between this case and the more usual types of self-similarity, where diffusion plays significant role, are discussed.

Key words: buoyancy, shear, similarity, turbulence

1. Introduction

Self-similarity solutions are frequently encountered in systems where diffusion (or generally, dissipation) plays an essential role [1]. This role is to destroy the memory of the system about the details of initial conditions and continuously destroy the memory of the details of random perturbations occurring during the dynamics. It can be said that, when an attracting self-similarity regime exists, it is the diffusion that drives the system to the attractor. In this work we analyze a less common situation where self-similarity emerges in a dissipative system after the diffusion has virtually decayed.

Consider two half-spaces of fluid having different velocities and stable density difference (Figure 1). Due to the velocity shear, turbulence starts developing and expanding (entraining) symmetrically upward and downward. Because of the stable stratification, the entrainment is suppressed by buoyancy forces. Such a process is interesting as a model of a layered structure in the ocean thermocline, and may also be useful in approximations of the mixing of an oil spill in the ocean or river with underneath water flows. Our primary purpose is, however, not to model precisely a particular case of fluid mechanics but rather to investigate fundamentals of self-similarity, identify its type and analyze differences from more "usual" cases.

Although the above process may look purely notional, it can be simulated in laboratory. In experiments [2,3] steady flows of gases were separated by a barrier. The flows meet each other at the tip of the barrier where turbulence starts developing. It was observed that the turbulent layer has sharp boundaries, and the thickness of the layer increases downstream. The spatial coordinate, x, directed downstream can be linked to the time in our notional situation, t, as $x = u_c t$, where u_c is the average velocity of the two initial flows, $u_c = (u_1 + u_2)/2$; see [4]. By moving with the average velocity an observer will see a time-dependent local thickness of the turbulent layer, quite similar to the time-dependent entrainment in the flow depicted in Figure 1. Some theoretical estimates of averaged flow characteristics relating to

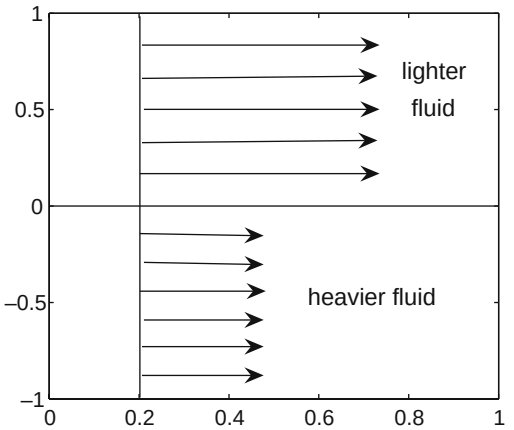

Figure 1. Initial flow.

the experiments were performed in [4,5]; however, no solutions were obtained for the whole time period, that is, until the turbulence decays completely.

We will use a short version of the K-ℓ model of turbulence based on a simple closing assumption about the spatial scale of turbulence. For the horizontally uniform (statistically) turbulent layer the model is written in the form (see [6], [1, Sections 10.2.2 and 11.3], [7]):

$$\partial_t K = \gamma_1 \partial_z (\ell \sqrt{K} \partial_z K) - \frac{\gamma K^{3/2}}{\ell} + \gamma_2 \ell \sqrt{K} (\partial_z u)^2 + \gamma_3 \ell \sqrt{K} (\partial_z \theta), \tag{1}$$

$$\partial_t u = \partial_z (\ell \sqrt{K} \partial_z u), \qquad \partial_t \theta = \gamma_4 \partial_z (\ell \sqrt{K} \partial_z \theta), \tag{2, 3}$$

where $K(z,t)$ is the turbulent energy, that is, ensemble-averaged kinetic energy of turbulent pulsations per mass unit; z is the upward-directed transverse coordinate; $\theta(z,t)$ is the averaged buoyancy defined as $\theta = g\rho(z,t)/\rho_0$, where g is the gravitational acceleration, ρ is the averaged density, and ρ_0 is the reference density; ℓ is the spatial scale of turbulence. Hereafter we assume $\gamma_1 = \gamma_2 = \gamma_3 = \gamma_4 = 1$ and $\gamma \approx 0{\cdot}06$; see [1, p. 281]. Note, however, that specific values of these constants will not be of principle significance.

In the right-hand side of the energy-balance equation (1) the terms express, from the left, the diffusion of the energy due to velocity pulsations, dissipation into heat, production by the velocity shear, and expenditure on work against the buoyancy forces. Equations (2) and (3) express the turbulent diffusion of the momentum and buoyancy.

To close system (1)–(3) we should somehow specify the spatial scale ℓ. Suggest, similarly to [1, p. 292], that the turbulent diffusion is predominantly due to large turbulent vortices with sizes comparable to the thickness of the layer. Accordingly, the scale ℓ will be proportional to the thickness denoted $2h(t)$:

$$\ell(t) = \mu h(t)\,, \tag{4}$$

where μ is a constant coefficient. Thus, the scale ℓ will be a function of time only. Note that $h(t)$ is a characteristic of a global solution; this renders this version of the K-ℓ model nonlocal.

Initial conditions for the velocity and buoyancy have the following step-like form:

$$u(z,0) = \begin{cases} u_1 & \text{for } z > \varepsilon \\ u_0(z) & \text{for } -\varepsilon < z < \varepsilon \\ u_2 & \text{for } z < -\varepsilon\,; \end{cases} \qquad \theta(z,0) = \begin{cases} \theta_1 & \text{for } z > \varepsilon \\ \theta_0(z) & \text{for } -\varepsilon < z < \varepsilon \\ \theta_2 > \theta_1 & \text{for } z < -\varepsilon\,. \end{cases} \tag{5, 6}$$

Here the parameter ε defines a narrow initial layer only introduced for the sake of smooth initial conditions in the numerical experiments. When ε tends to zero, the initial profiles become ideal steps.

To formulate an initial condition for the turbulent energy, observe from (1) that, in order to start the dynamics, it is sufficient to seed some non-zero amount of the energy; the energy will then be pumped up by the shear term. We assume

$$K(z,0)=\begin{cases}0 & \text{for} \quad z>\varepsilon\\ K_0(z) & \text{for} \quad -\varepsilon<z<\varepsilon\\ 0 & \text{for} \quad z<-\varepsilon\,.\end{cases} \tag{7}$$

In (5)–(7) $u_0(z)$, $\theta_0(z)$ and $K_0(z)$ are some initial profiles that have no effect on the solution when $\varepsilon\to 0$.

Due to the symmetry properties of the initial conditions (5)–(7), the profile of the turbulent energy at $t>0$ will be symmetric with respect to $z=0$ and the profiles of the velocity and buoyancy will be anti-symmetric. Hence, it will suffice to consider only half of the turbulent layer, say $z\geq 0$, provided that appropriate conditions are formulated at the middle point $z=0$.

By symmetry, such a condition for the turbulent energy is that of zero flux,

$$\partial_z K|_{z=0}=0\,. \tag{8}$$

The values of the velocity and buoyancy in the middle of the layer must equal their respective average values between the half-spaces. Note here that the dynamical equations only involve gradients of u and θ; hence, we may subtract constant values from u and θ and transform to the new variables,

$$u(x,t)\to u(x,t)-\frac{u_1+u_2}{2}\,,\quad \rho(x,t)\to\rho(x,t)-\frac{\rho_1+\rho_2}{2}$$

with the dynamic equations remaining unchanged. Therefore, for the shifted velocity and buoyancy, the boundary conditions at $z=0$ become simply

$$u(0,t)=0\,,\quad \theta(0,t)=0\,. \tag{9}$$

Note that for $z>0$ the buoyancy is negative since the upper half-space has a lower density. However, in analogy to an always positive velocity, it will be convenient to deal with a positively valued buoyancy. So we will multiply the buoyancy by (-1). Accordingly, to restore the damping effect, the sign of buoyancy term in (1) will be changed to "minus".

On the turbulent front contacting with the unperturbed laminar flow the turbulent energy vanishes; hence

$$K[h(t),t]=0\,, \tag{10}$$

and the shifted velocity and buoyancy are equal to their respective unperturbed values, *viz*.

$$u[h(t),t]=\frac{u_1-u_2}{2}\equiv U\,,\quad \theta[h(t),t]=\frac{\theta_2-\theta_1}{2}\equiv gA\,. \tag{11}$$

In (11) A stands for the Atwood number measuring the initial buoyancy jump. Choosing the reference density to be the average of the unperturbed densities, $\rho_0=(\rho_1+\rho_2)/2$, we obtain from (11): $A=(\rho_2-\rho_1)/(\rho_1+\rho_2)$, which is the conventional expression for the Atwood number. Note that U and gA in (11) are halves of the total change of the velocity and buoyancy across the turbulent layer.

Lastly, the flux of the turbulent energy equals zero on the front:

$$\sqrt{K}\,\partial_z K\Big|_{z=h(t)}=0\,. \tag{12}$$

2. Qualitative analysis and numerical experiment

As a first step, evaluate the terms in the energy equation (1) according to their orders of magnitude and omitting constant coefficients. Replacing the derivatives by finite differences and assuming $\Delta K \sim K_0$, with K_0 being the maximum energy in the turbulent layer, $\Delta z \sim h$ and $\ell \sim h$, we have

$$\text{diffusion term} \sim \frac{K_0^{3/2}}{h}, \quad \text{shear term} \sim \frac{K_0^{1/2}}{h}, \quad \text{buoyancy term} \sim K_0^{1/2}.$$

During the early stage of the dynamics, the thickness $h(t)$ is small; therefore, the production shear term prevails over the buoyancy term. As a result, the turbulent energy increases and the turbulent layer expands due to the diffusion. As $h(t)$ gets larger, the buoyancy term becomes larger in absolute value than the shear term. Being suppressed by buoyancy, the turbulent energy must then decay. When this occurs the diffusion term, which is of higher order in K_0, becomes small in comparison with the buoyancy and shear terms.

We solved system (1)–(4) subject to the initial and boundary conditions (5)–(12) numerically, using U as the velocity scale, gA as the buoyancy scale, U^2 as the turbulent energy scale, $U^2/(gA)$ as the spatial scale, and $U/(gA)$ as the time scale. The value of the parameter ε was chosen small enough, so that neither ε nor the form of the initial profiles $u_0(z)$, $\theta_0(z)$ and $K_0(z)$ had any long-term effect on the solution. The original equations were non-dimensionalized and discretized using finite differences and the system of ODEs was solved in time with the MATLAB solver `DAE2`; see [8].

Note that, in non-dimensional form, the velocity and buoyancy coincide at all times, as their evolution equations and boundary and initial conditions are the same (assuming $\varepsilon \to 0$). Therefore, of the two quantities we will consider only one, the velocity.

The relative decay of the diffusion term is clearly seen in Figures 2–3. At about $t = 16$ the numerical experiment was hampered by numerical instability in the vicinity of the front, which is visible on the last plot in Figure 3. For this reason we did not compute further in time.

Nonetheless, the results shown here indicate that: (a) the diffusion term becomes relatively small and (b) when this occurs, the shear and buoyancy terms do not counterbalance each other exactly, with the buoyancy term being substantially larger in absolute value. With diffusion excluded, the expansion of the turbulent layer must cease.

Very recently computations were performed [9] for the whole time range, that is, until the turbulence decays to zero. They confirmed both effects (a) and (b) (we will comment on [9] in Section 3.2).

3. Self-similarity regimes and their stability

3.1. Finite turbulent layer

Since the turbulent layer cannot expand infinitely in space, we may seek a solution describing a regime where the layer reaches finite maximum thickness, at which moment the turbulent energy decays to zero exactly at all points. It will then be interesting to analyze the stability of such a regime.

Assuming that the details of the initial distributions $u_0(z)$, $\theta_0(z)$ and $K_0(z)$ (see (5)–(7)) in the initially narrow layer are insignificant, we state that the quantities of interest, namely

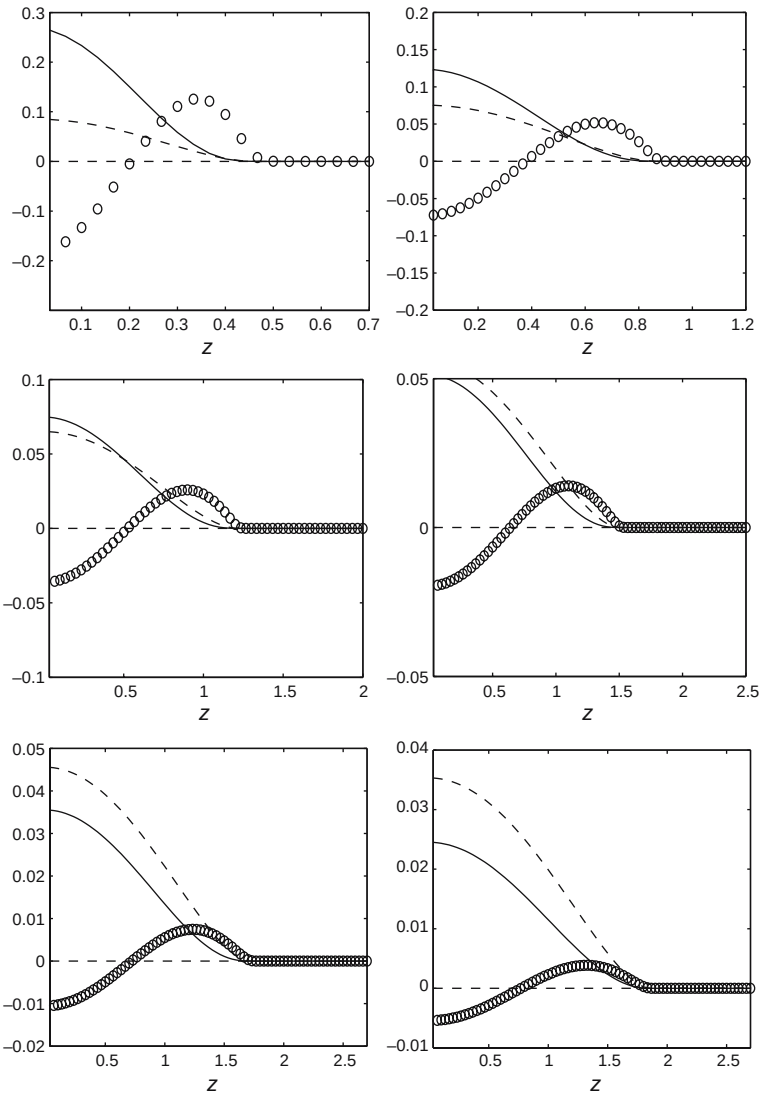

Figure 2. Comparison of the terms in energy balance (1) as the turbulent layer expands ($t = 2$, 4, 6, 8, 10, 12). Solid line – the shear; dashed line – the buoyancy; circles – the diffusion. $\mu = 0{\cdot}2$.

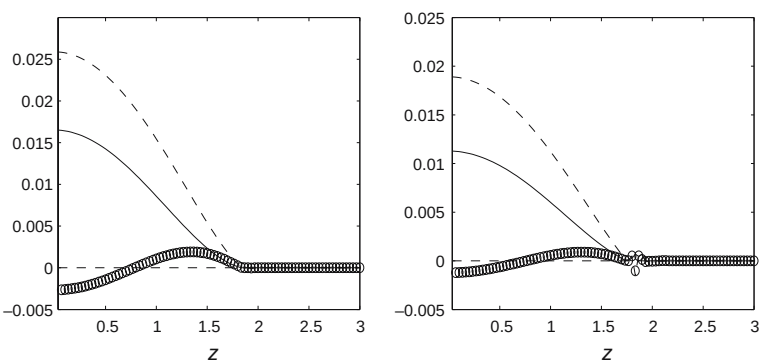

Figure 3. Continued from Figure 2 ($t = 14$, 16).

$$u\,(\mathrm{cm/s}),\quad \theta\,(\mathrm{cm/s^2}),\quad K\,(\mathrm{cm^2/s^2}),\quad h\,(\mathrm{cm}),$$

$$\text{depend on} \tag{13}$$

$$U\,(\mathrm{cm/s}),\quad gA\,(\mathrm{cm/s^2}),\quad z\,(\mathrm{cm}),\quad t\,(\mathrm{s}).$$

Among the independent variables here, two have independent dimensionalities, for example, U and gA. We transfer now to non-dimensional variables in (13) by non-dimensionalizing all the quantities, using U and gA, and find that

$$\frac{u}{U},\quad \frac{\theta}{gA},\quad \frac{K}{U^2},\quad \frac{hgA}{U^2}\quad \text{depend on}\quad \frac{zgA}{U^2},\quad \frac{tgA}{U}. \tag{14}$$

Now seek a solution in the form

$$\frac{h(t)gA}{U^2} = h_* - \beta\left(t_* - \frac{tgA}{U}\right)^{\lambda}, \tag{15}$$

where h_*, t_*, β and λ are positive non-dimensional constants. Expression (15) corresponds to times close to the final moment t_* when the layer has maximum thickness h_*:

$$\frac{h(t)gA}{U^2} \to h_* \quad \text{when} \quad \frac{tgA}{U} \to t_*. \tag{16}$$

Denote the time interval left until the moment t_* by

$$\tau \equiv t_* - \frac{tgA}{U} \to 0.$$

Instead of the non-dimensional coordinate zgA/U^2, let us consider a normalized coordinate obtained by dividing this by the non-dimensional combination $h(t)gA/U^2$:

$$\xi = \frac{z}{h(t)},\quad \text{so that conveniently}\quad 0 \le \xi \le 1. \tag{17}$$

As $\tau \to 0$, the velocity approaches the limiting profile,

$$\frac{u}{U} \to P(\xi). \tag{18}$$

As was emphasized in the previous section, the non-dimensional velocity and buoyancy coincide, therefore

$$\frac{\theta}{gA} \to P(\xi). \tag{19}$$

The turbulent energy turns zero at the moment t_*, whence we seek K in the form

$$\frac{K}{U^2} = \left(t_* - \frac{tgA}{U}\right)^{\alpha}\Phi(\xi). \tag{20}$$

Substituting (16), (17), (18), (19) and (20) in (1)–(4) and rearranging we have:

$$-\alpha\tau^{\alpha-1}\Phi - \frac{\lambda\beta}{h_*}\tau^{\alpha+\lambda-1}\xi\frac{\mathrm{d}\Phi}{\mathrm{d}\xi} = \frac{\mu}{h_*}\tau^{3\alpha/2}\frac{\mathrm{d}}{\mathrm{d}\xi}\left(\sqrt{\Phi}\frac{\mathrm{d}\Phi}{\mathrm{d}\xi}\right) - \frac{\gamma}{\mu h_*}\tau^{3\alpha/2}\Phi^{3/2} + \frac{\mu}{h_*}\tau^{\alpha/2}\sqrt{\Phi}\left(\frac{\mathrm{d}P}{\mathrm{d}\xi}\right)^2 - \mu\tau^{\alpha/2}\sqrt{\Phi}\frac{\mathrm{d}P}{\mathrm{d}\xi}, \tag{21}$$

$$-\lambda\beta\tau^{\lambda-1}\xi\frac{\mathrm{d}P}{\mathrm{d}\xi} = \mu\tau^{\alpha/2}\frac{\mathrm{d}}{\mathrm{d}\xi}\left(\sqrt{\Phi}\frac{\mathrm{d}P}{\mathrm{d}\xi}\right). \tag{22}$$

The boundary conditions complementing (21)–(22) result from (8)–(12), (18) and (20):

$$\sqrt{\Phi}\frac{\mathrm{d}\Phi}{\mathrm{d}\xi}\bigg|_{\xi=1}=0\,,\quad \frac{\mathrm{d}\Phi}{\mathrm{d}\xi}\bigg|_{\xi=0}=0\,,\quad \Phi(1)=0\,, \tag{23}$$

$$P(0)=0\,,\quad P(1)=1\,. \tag{24}$$

In order for (22) to be an ordinary differential equation, the terms with τ should cancel out. This happens when

$$\lambda-1=\frac{\alpha}{2}\,. \tag{25}$$

Taking into account (25), we see that the second term in the left-hand side of (21) is of the order $\tau^{\alpha+\lambda-1}=\tau^{3\alpha/2}$, and the first two terms in the right-hand side are also of the order $\sim \tau^{3\alpha/2}$. As $\tau\to 0$ these terms can be neglected in comparison with the lower-order terms containing $\tau^{\alpha/2}$. Thus, Equation (21) reduces to

$$-\alpha\tau^{\alpha-1}\Phi=\frac{\mu}{h_*}\tau^{\alpha/2}\sqrt{\Phi}\left(\frac{\mathrm{d}P}{\mathrm{d}\xi}\right)^2-\mu\,\tau^{\alpha/2}\sqrt{\Phi}\frac{\mathrm{d}P}{\mathrm{d}\xi}\,. \tag{26}$$

In order for (26) to be an ODE, the parameter τ must disappear, which occurs if

$$\alpha-1=\alpha/2\,,\quad \text{therefore}\quad \alpha=2\,. \tag{27}$$

Equation (25) then gives

$$\lambda=2\,. \tag{28}$$

Substituting (25) and (27) in (22) and (26), we get two equations to determine $P(\xi)$ and $\Phi(\xi)$:

$$-2\sqrt{\Phi}=\frac{\mu}{h_*}\left(\frac{\mathrm{d}P}{\mathrm{d}\xi}\right)^2-\mu\frac{\mathrm{d}P}{\mathrm{d}\xi}\,,\qquad -\frac{2\beta}{\mu}\xi\frac{\mathrm{d}P}{\mathrm{d}\xi}=\frac{\mathrm{d}}{\mathrm{d}\xi}\left(\sqrt{\Phi}\frac{\mathrm{d}P}{\mathrm{d}\xi}\right)\,. \tag{29}$$

Denoting

$$\frac{\mathrm{d}P(\xi)}{\mathrm{d}\xi}=R(\xi), \tag{30}$$

we rewrite (29) as

$$-2\sqrt{\Phi}=\frac{\mu}{h_*}R^2-\mu R\,,\qquad -\frac{2\beta}{\mu}\xi R=\frac{\mathrm{d}}{\mathrm{d}\xi}\left(\sqrt{\Phi}R\right)\,. \tag{31, 32}$$

Substituting $\sqrt{\Phi}$ from (31) in (32) yields the 2nd-order ODE for the function $R(\xi)$:

$$-\frac{2\beta}{\mu}\xi R=\frac{\mathrm{d}}{\mathrm{d}\xi}\left[\left(\frac{\mu}{2}R-\frac{\mu}{2h_*}R^2\right)R\right]\,. \tag{33}$$

The solution of (33) is

$$R(\xi)=\frac{2h_*}{3}\left[1-\sqrt{1-\frac{3}{2h_*}\left(C-\frac{2\beta}{\mu^2}\xi^2\right)}\right]\,. \tag{34}$$

At the front $\Phi(1)=0$ (see (23)); hence (31) suggests that either $R(1)=0$ or $R(1)=h_*$. The numerical experiments show that, during the expansion stage, the velocity has zero gradient on the front, whence we assume

$$R(1)=0\,. \tag{35}$$

The conditions (35) and (34) determine the constant C:

$$C = \frac{2\beta}{\mu^2}, \tag{36}$$

so that (34) becomes

$$R(\xi) = \frac{2h_*}{3}\left[1 - \sqrt{1 - \frac{3\beta}{h_*\mu^2}(1-\xi^2)}\right]. \tag{37}$$

The expression under the square root must be positive for all ξ including $\xi = 0$; therefore

$$1 - \frac{3\beta}{h_*\mu^2} > 0. \tag{38}$$

The velocity profile is derived from (30) and (37):

$$P(\xi) = \int_0^\xi R(\xi')\,\mathrm{d}\xi' = \frac{2h_*}{3}\xi - \frac{2h_*}{3}\left[\frac{\xi}{2}\sqrt{1-b+b\xi^2} + \frac{1-b}{2\sqrt{b}}\log\left(\xi\sqrt{\frac{b}{1-b}} + \sqrt{1+\frac{b}{1-b}\,\xi^2}\right)\right], \tag{39}$$

where, in view of (38),

$$b = \frac{3\beta}{h_*\mu^2} < 1. \tag{40}$$

The profile of the turbulent energy is determined by (31) and (37):

$$\Phi(\xi) = \frac{1}{4}\mu^2 R^2(\xi)\left(1 - \frac{R(\xi)}{h_*}\right)^2. \tag{41}$$

In view of Equation (40) it is easy to show that

$$P(1) = \frac{2h_*}{3}\left(\frac{1}{2} - \frac{1-b}{2\sqrt{b}}\log\frac{1+\sqrt{b}}{\sqrt{1-b}}\right) < \frac{h_*}{3}. \tag{42}$$

From (42) and the boundary condition $P(1) = 1$ we get the following useful estimate

$$h_* > 3. \tag{43}$$

Figure 4 shows the solution for one value of h_* satisfying condition (43).

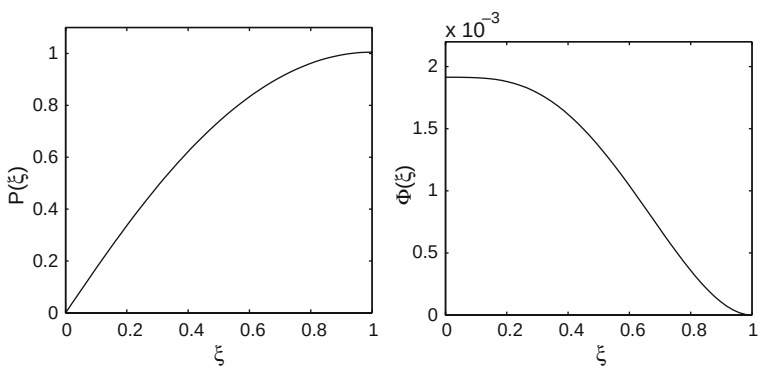

Figure 4. Self-similarity profiles of the velocity (39) and turbulent energy (41) for $h_* = 3{\cdot}5$, $\beta = 1{\cdot}09 \times 10^{-2}$, $\mu = 0{\cdot}2$.

Once the similarity solution is found, it is interesting to investigate its stability. Consider the energy balance (1). The derivative $\partial_z u$ at the front, $z=h(t)$, is equal to zero. In the neighbourhood of this point the quadratic term, $(\partial_z u)^2$, is small compared to the linear term, $\partial_z \theta \sim \partial_z u$. Hence the equation simplifies to $\partial_t K \sim -\sqrt{K}\partial_z u$ or $\partial_t \sqrt{K} \sim -\partial_z u < 0$. Consequently $\sqrt{K}$ must decrease with time and so must the value of K, as is also a consequence of (20). Suppose that a perturbation occurs and the velocity profile becomes slightly steeper than it should be according to the similarity solution. In order to restore the flatter slope, a stronger mixing is required, that is, a stronger supply of the turbulent energy. However, this cannot occur, as the energy evolves in the opposite direction: due to the perturbation $(-\partial_z u)$ would become more negative, and thus $\sqrt{K}$ will decay even faster. These arguments indicate that the obtained similarity solution is unstable.

3.2. Shrinking turbulent layer

We therefore seek a different form of similarity. Assume now that the turbulent layer shrinks:

$$\frac{h(t)gA}{U^2} = \chi\left(t_* - \frac{tgA}{U}\right)^{\lambda}, \quad \lambda > 0, \tag{44}$$

where t_* is the moment when the layer turns to a point, and χ and λ are constants. Apparently the value of t_* is different from the one in the previous section. The velocity and buoyancy (which, as we remember, coincide) are sought in the self-similar form

$$\frac{u}{U} = \frac{\theta}{gA} = \left(t_* - \frac{tgA}{U}\right)^{\omega} P(\xi), \quad \omega > 0, \tag{45}$$

where

$$\xi = \frac{z}{h(t)}, \quad 0 \le \xi \le 1.$$

The time-dependent multiplier in (45) reflects the geometric effect of a diminishing boundary value of the velocity on the front as it moves toward the point $z=0$. Note in this regard that the turbulent layer shrinks inside the region that is already mixed during the expansion stage. Therefore, the front of turbulence moves back to the middle point $z=0$ through the area where a non-zero gradient of the velocity (and buoyancy) already exists. This means that the value of the velocity on the front, $z=h(t)$, decreases with time before turning exactly zero at the moment t_*. This decrease can be asymptotically described by some power law as reflected by (45): on the front we have $\xi=1$ and thus $u/U = (t_* - tgA/U)^{\omega} P(1)$.

The turbulent energy is sought in the form

$$\frac{K}{U^2} = \left(t_* - \frac{tgA}{U}\right)^{\alpha} \Phi(\xi), \quad \alpha > 0. \tag{46}$$

Using the earlier notation

$$\tau \equiv t_* - \frac{tgA}{U}$$

we transform the energy equation (1) to

$$-\alpha\tau^{\alpha-1}\Phi + \lambda\tau^{\alpha-1}\xi\frac{\mathrm{d}\Phi}{\mathrm{d}\xi} = \frac{\mu}{\chi}\tau^{3\alpha/2-\lambda}\frac{\mathrm{d}}{\mathrm{d}\xi}\left(\sqrt{\Phi}\frac{\mathrm{d}\Phi}{\mathrm{d}\xi}\right) - \frac{\gamma}{\mu\chi}\tau^{3\alpha/2-\lambda}\Phi^{3/2} + \frac{\mu}{\chi}\tau^{\alpha/2+2\omega-\lambda}\sqrt{\Phi}\left(\frac{\mathrm{d}P}{\mathrm{d}\xi}\right)^2 - \mu\tau^{\alpha/2+\omega}\sqrt{\Phi}\left(\frac{\mathrm{d}P}{\mathrm{d}\xi}\right). \tag{47}$$

In (47) the two non-stationary terms on the left are of the same order in τ. They are also of the same order as the shear and buoyancy terms, provided that the powers of τ are equal:

$$\alpha - 1 = \alpha/2 + 2\omega - \lambda = \alpha/2 + \omega \,. \tag{48}$$

From (48) we find

$$\omega = \lambda \,, \quad \text{and} \quad \alpha = 2(\lambda + 1) \,. \tag{49}$$

Taking into account (49), we see that, in agreement with the numerical results shown in Figure 2–3, the diffusion and heat-dissipative terms in the turbulent energy equation become relatively small as $\tau \to 0$ because

$$\tau^{2\lambda+3} \equiv \tau^{3\alpha/2-\lambda} \ll \tau^{\alpha-1} \equiv \tau^{2\lambda+1} \,.$$

Hence, Equation (47) simplifies to

$$-\alpha\Phi + \lambda\xi \frac{\mathrm{d}\Phi}{\mathrm{d}\xi} = \frac{\mu}{\chi}\sqrt{\Phi}\left(\frac{\mathrm{d}P}{\mathrm{d}\xi}\right)^2 - \mu\sqrt{\Phi}\left(\frac{\mathrm{d}P}{\mathrm{d}\xi}\right) \,. \tag{50}$$

Upon transformation to ξ, the momentum equation (2) assumes the form

$$-\omega\tau^{\omega-1}P + \lambda\tau^{\omega-1}\xi\frac{\mathrm{d}P}{\mathrm{d}\xi} = \frac{\mu}{\chi}\tau^{\alpha/2-\lambda+\omega}\frac{\mathrm{d}}{\mathrm{d}\xi}\left(\sqrt{\Phi}\frac{\mathrm{d}P}{\mathrm{d}\xi}\right) \,. \tag{51}$$

Since $\tau \to 0$,

$$\tau^{\lambda+1} \equiv \tau^{\alpha/2-\lambda+\omega} \ll \tau^{\omega-1} \equiv \tau^{\lambda-1} \,;$$

therefore the diffusion in (51) can be neglected and we get

$$-\omega P + \lambda\xi\frac{\mathrm{d}P}{\mathrm{d}\xi} = 0 \,. \tag{52}$$

Solving (52) gives $P(\xi) = C\xi^{\omega/\lambda}$. Further, the gradient of the velocity in the middle of the layer, $\xi = 0$, must be finite (not zero and not infinity) as a result of the mixing during the expansion stage. During the contracting stage the gradient should remain finite. This dictates that the velocity profile must be linear (*i.e.*, $\omega = \lambda$):

$$P(\xi) = C\xi \tag{53}$$

(which is equivalent to $u = Cz/h(t)$, $0 \le z \le h(t)$ in dimensional form). Due to (53) the energy balance (50) reduces to

$$\lambda\xi\frac{\mathrm{d}\Phi}{\mathrm{d}\xi} = \left(\frac{\mu}{\chi}C^2 - \mu C\right)\sqrt{\Phi} + 2(\lambda+1)\Phi \,. \tag{54}$$

Subject to the boundary condition $\Phi(1) = 0$, the solution of (54) is

$$\Phi(\xi) = \frac{\mu^2 C^2}{4(\lambda+1)^2}\left(1 - \frac{C}{\chi}\right)^2\left(1 - \xi^{\frac{\lambda+1}{\lambda}}\right)^2 \,. \tag{55}$$

To determine λ, note that the diffusion term is asymptotically small during the layer's contraction; however, this term remains non-zero until the very last moment t_*. Therefore, there

is still the requirement that the energy flux is equal to zero at $\xi = 0$. Solution (55) meets this requirement automatically for any λ because

$$\frac{\lambda+1}{\lambda} > 1 .$$

However, there is another requirement that $\Phi(\xi)$ be expandable into a Taylor series around the point $\xi = 0$, because it is merely an internal point of the turbulent layer, so $\Phi(\xi)$ must be as smooth there as it is in other points. This requires the power of ξ in (55) to be an integer number. The smallest integer value of $(\lambda+1)/\lambda$ is 2, therefore

$$\lambda = 1 . \tag{56}$$

In view of (56) the turbulent energy (55) is simplified to the form

$$\Phi(\xi) = \frac{\mu^2 C^2}{16}\left(1 - \frac{C}{\chi}\right)^2 \left(1 - \xi^2\right)^2 . \tag{57}$$

The velocity gradient C cannot be determined from the self-similarity problem alone and depends on the previous dynamics.

From (56) and (49) we obtain

$$\alpha = 4 . \tag{58}$$

Solutions (53), (57) are shown in Figure 5. Observe from (44), (56) that the thickness of the turbulent layer diminishes linearly against the remaining time,

$$h(\tau) \sim \tau , \tag{59}$$

and, due to (58), the turbulent energy (46) decays as the fourth power of the remaining time,

$$K(\tau) \sim \tau^4 . \tag{60}$$

Recent numerical experiments [9] confirmed the laws (59), (60), as well as the linear shape of the velocity/buoyancy profile (53) and parabolic shape of the square root of the energy, $\sqrt{K} \sim \sqrt{\Phi(\xi)} \sim 1 - \xi^2$; see (57). In the computations, instead of the "usual" non-dimensional time $t_1 = tgA/U$, the scaled time, $\hat{t}_1$ was used, such that $\mathrm{d}\hat{t}_1 = \mathrm{d}t_1 \ell_1(t_1)$, where $\ell_1 = \ell g A/U^2$ is the non-dimensional scale of turbulence. It was found that, for $\mu = 0{\cdot}2$, the layer starts shrinking at $\hat{t}_1 \approx 2$ and reduces to a point at $\hat{t}_1 \approx 3{\cdot}42$.

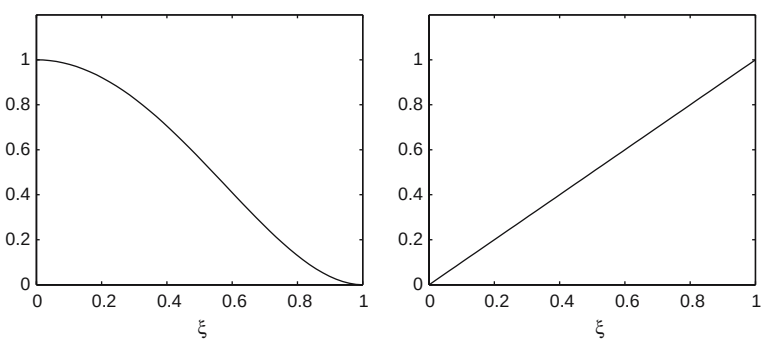

Figure 5. Self-similarity profiles for shrinking turbulent layer. Left: turbulent energy, $\Phi(\xi)16/[\mu^2 C^2(1 - C/\chi)^2]$, right: velocity, $P(\xi)/C$ (both normalized).

Let us now analyze the stability of the regime. The arguments we used previously to show instability of the finite layer are no longer applicable. As the turbulent layer contracts, the section of the velocity/buoyancy profile inside the layer approaches a linear shape for a simple geometric reason: any smooth curve is nearly linear on a short distance (from the point $\xi = 0$ in our case). Any perturbation that may affect the dynamics is eventually left outside the region of interest, which is the turbulent layer. In this situation no returning mechanism is required.

The fact that in [9] it was the shrinking layer that was observed, and not the finite layer, supports the arguments on stability.

4. Discussion and conclusion

A self-similarity solution is just one of the many solutions of a nonlinear problem. However, such a solution is often important as an attractor for other solutions. The self-similarity is normally uncovered by reducing original PDEs to ODEs and applying boundary conditions. It then occurs that the solution only satisfies all the conditions for some special values – eigenvalues – of power exponents in similarity variables, such as the power exponent of time (see [1], in particular the example on p. 292 therein).

In our problem the situation is somewhat different. Upon removal of the diffusion term, the energy balance assumes the form where there are no other solutions except the self-similar one.

To illustrate this point, consider the original energy equation (non-dimensional), which is a counterpart of (50), only without *a priori* assumptions of the form of the solution:

$$\frac{\partial K_1}{\partial t_1} = \mu h_1 \sqrt{K_1} \left[\left(\frac{\partial u_1}{\partial z_1} \right)^2 - \frac{\partial \theta_1}{\partial z_1} \right]. \tag{61}$$

Here the subscript 1 indicates non-dimensional quantities. As we argued earlier, due to the diffusion during the expansion stage, the velocity and buoyancy in the middle of the turbulent layer must have finite non-zero gradients. As the layer shrinks later, these profiles become virtually linear:

$$\frac{\partial u_1}{\partial z_1} = \frac{\partial \theta_1}{\partial z_1} = \frac{1}{\chi} \frac{\mathrm{d}P}{\mathrm{d}\xi} = \frac{C}{\chi}. \tag{62}$$

Substituting (62) in (61), we obtain

$$\frac{\partial K_1}{\partial t_1} = -\mu h_1(t_1) \sqrt{K_1} \left[\frac{C}{\chi} - \left(\frac{C}{\chi} \right)^2 \right], \quad \text{where} \quad \frac{C}{\chi} - \left(\frac{C}{\chi} \right)^2 > 0. \tag{63}$$

Rewrite (63) in terms of $k = \sqrt{K_1}$:

$$\frac{\partial k}{\partial t_1} = -\frac{C}{2\chi} \left(1 - \frac{C}{\chi} \right) \mu h_1(t_1). \tag{64}$$

Equation (64) is an ODE for $k_1(t_1)$ with the unknown function $h_1(t_1)$. The layer's thickness, $h_1(t_1)$, decreases according to a power law:

$$h_1(t_1) = \chi (t_* - t_1)^{\lambda}. \tag{65}$$

Inserting (65) into (64) and integrating, we have

$$k(z_1, t_1) = -\frac{C}{2\chi} \left(1 - \frac{C}{\chi} \right) \mu \int h_1(t_1)\, \mathrm{d}t_1 + g(z_1) = \frac{C}{2} \left(1 - \frac{C}{\chi} \right) \frac{\mu}{\lambda + 1} (t_* - t_1)^{\lambda + 1} + g(z_1), \tag{66}$$

where $g(z_1)$ is a constant of integration. Now apply the boundary condition

$$k|_{z_1=h_1(t_1)}=0$$

to (66) and take into account (65):

$$\frac{C}{2}\left(1-\frac{C}{\chi}\right)\frac{\mu}{\lambda+1}(t_*-t_1)^{\lambda+1}+g\left[\chi(t_*-t_1)^{\lambda}\right]=0\,. \tag{67}$$

From (67), denoting $\chi(t_*-t_1)^{\lambda}$ by z_1, we determine the function $g(z_1)$:

$$g(z_1)=-\frac{C}{2}\left(1-\frac{C}{\chi}\right)\frac{\mu}{\lambda+1}\left(\frac{z_1}{\chi}\right)^{\frac{\lambda+1}{\lambda}}\,.$$

Consequently, from (66):

$$\begin{aligned}k(z_1,t_1)&=\frac{C}{2}\left(1-\frac{C}{\chi}\right)\frac{\mu}{\lambda+1}\left[(t_*-t_1)^{\lambda+1}-\left(\frac{z_1}{\chi}\right)^{\frac{\lambda+1}{\lambda}}\right]\\&=\frac{C}{2}\left(1-\frac{C}{\chi}\right)\frac{\mu}{\lambda+1}(t_*-t_1)^{\lambda+1}\left[1-\left(\frac{z_1}{\chi(t_*-t_1)^{\lambda}}\right)^{\frac{\lambda+1}{\lambda}}\right]\\&=(t_*-t_1)^{\lambda+1}\frac{\mu C}{2(\lambda+1)}\left(1-\frac{C}{\chi}\right)\left(1-\xi^{\frac{\lambda+1}{\lambda}}\right)\,.\end{aligned} \tag{68}$$

Formula (68) describes the self-similarity regime. Taking into account that $\alpha=2(\lambda+1)$ and $k=\sqrt{K_1}=\tau^{\alpha/2}\sqrt{\Phi}$, we may easily verify that (68) is equivalent to (55).

It is interesting to look at the role of the diffusion in the formation of the self-similarity. In contrast to "usual" situations, the diffusion term is missing from the energy equation. However, the diffusion does have a consequence—it justifies the selection of a unique solution, (57), from a variety of solutions, (55), via the smoothness condition at $z=0$. But should this requirement be imposed while the diffusion term is not present in the equation? The answer is yes because the diffusion was substantial during the expansion stage when the smooth energy profile was created. Thereafter the profile remains smooth during the shrinking stage.

It is also interesting to classify the self-similarity. According to the classification [1, Chapter 5] all self-similarity regimes are grouped in two classes: complete and incomplete similarity. For a complete similarity, a dimensional analysis is sufficient to determine the power exponents of the similarity variables. A textbook example of such a kind of similarity is heat propagation from an instantaneous point source. The rate of temperature decrease at the source location, $T\sim q/\sqrt{Dt}\sim 1/\sqrt{t}$ (q is the total amount of heat measured in K·cm, D is the diffusion coefficient measured in cm^2/s) follows immediately from the dimensional analysis as soon as we realize that T depends on q, D and t. For an incomplete similarity, a dimensional analysis is not sufficient to establish the power exponents. In such cases the power exponents are obtainable from nonlinear eigenvalue problems as we mentioned above (for a detailed description and examples see [1]).

This also applies to our problem, however, with some alterations. As is typical for incomplete similarity, the power exponent α in the expression for the turbulent energy (46) cannot be determined from a dimensional analysis. This parameter is connected to λ through (49) and λ appears to be the eigenvalue governed by the boundary condition at $\xi=0$. In most cases of incomplete similarity the boundary condition analogous to zero flux of the turbulent energy at $\xi=0$ would be sufficient to determine the eigenvalue. In our case this is not so because

the self-similarity solution (55) satisfies this condition for any $\lambda > 0$. However, the additional requirement of smoothness of the energy profile at $\xi = 0$ selects a unique value of λ.

Lastly, we note that the velocity and buoyancy profiles formally belong to a complete similarity class as they are virtually stationary. We therefore have two types of similarity within one problem: quasi-incomplete similarity for K and complete for u and θ.

We considered an example of a system related to fluid mechanics, which asymptotically behaves in a self-similar manner without diffusion. This feature sets the situation apart from more typical cases of self-similarity where the diffusion is involved as an essential factor affecting the dynamics.

Specifically, an evolution of a turbulent layer has been analyzed between half-spaces of fluid having different velocities and densities. The turbulent layer expands during an initial stage of the evolution pumped up by velocity shear, but the expansion is eventually stopped by stable stratification. During the late stage of the evolution, the role of turbulent diffusion becomes negligible compared to the impact from shear and buoyancy.

Two possibilities of the final stage of the dynamics were analyzed: where the layer's thickness (a) increases up to some finite maximum value (Section 3.1), and (b) shrinks to zero (Section 3.2). It was found that regime (a) is unstable while regime (b) is stable and is therefore physically realistic. Unstable solutions are generally of marginal interest only and we did not investigate whether or not there are other unstable regimes apart from (a). Peculiarities of the similarity solution describing the stable regime have been discussed and compared to typical cases of complete and incomplete similarity.

Acknowledgement:

The author thanks S.A. Suslov for the advice on numerical experiments and valuable discussions.

References

1. G.I. Barenblatt, *Scaling, Self-similarity, and Intermediate Asymptotics*. Cambridge: Cambridge University Press (1996) 386 pp.
2. R.D. Mills, Numerical and experimental investigations of the shear layer between two parallel streams. *J. Fluid Mech*. 33 (1968) 591–616.
3. I. Wygnanski and H.E. Fiedler, The two-dimensional mixing region. *J. Fluid Mech*. 41 (1970) 327–361.
4. G.L. Brown and A. Roshko, On density effects and large structure in turbulent mixing layers. *J. Fluid Mech*. 64 (1974) 775–816.
5. A. Roshko, Structure of turbulent shear flows: a new look. *AIAA J*. 14 (1976) 1349–1357.
6. A.N. Kolmogorov, Equations of turbulent motion of incompressible fluid. *Izv. Akad. Nauk SSSR, Ser. Fiz*. 6 (1942) 56–58.
7. C.G. Speziale, Analytical methods for the development of Reynolds-stress closures in turbulence. *Ann. Rev. Fluid Mech*. 23 (1991) 107–157.
8. A.J. Roberts, *http://www.sci.usq.edu.au/staff/robertsa/*.
9. S.A. Suslov, private communication (2004).